DOI: 10.1002/chem.200902740

Induced Chiroptical Changes of a Water-Soluble Cryptophane by Encapsulation of Guest Molecules and Counterion Effects

Aude Bouchet,[a] Thierry Brotin,*[b] Dominique Cavagnat,[a] and Thierry Buffeteau*[a]

Dedicated to the memory of André Collet

Abstract: We report the synthesis of the water-soluble cryptophanol derivative **1** and the study of the chiroptical properties of its two enantiomers (>99% *ee*) by polarimetry, electronic circular dichroism (ECD), and vibrational circular dichroism (VCD). We show that cryptophanol **1** exhibits unusual chiroptical properties in water under basic conditions (pH>12). For instance, the shapes of the ECD and VCD spectra of **1** in water were strongly dependent on the nature of the alkali metal ions (Li^+, Na^+, K^+, Cs^+) surrounding the cryptophane and whether or not a guest molecule is present inside the cavity of the host. To the best of our knowledge, this is the first example in which the nature of these counterions governs the chiroptical properties of a host molecule. Moreover, specific ECD spectra were obtained depending on the size of the guest molecules. This makes **1** a good sensor for small neutral molecules in aqueous solvent. Finally, VCD experiments associated with DFT calculations show that the chiroptical changes can be directly correlated to the presence of charges close to the aromatic rings and with a conformational change of the alkyl chains upon encapsulation.

Keywords: chiroptical properties · circular dichroism · cryptophane · density functional calculations · host–guest systems

Introduction

Cryptophanes are nearly spherical cage molecules composed of two cyclotriveratrylene (CTV) bowls connected by three aliphatic linkers. The rigid bowl-shape structure of the cryptophane cavity generates a lipophilic cavity suitable for the encapsulation of small neutral molecules.[1] The specific molecular recognition is mainly determined by the internal volume of the cavity, which in turn is controlled by the length of the aliphatic linkers (81, 95, and 121 Å^3 for methoxy, ethoxy, and propoxy linkers, respectively).[1b] Thus, cryptophane derivatives can encapsulate a variety of guest molecules, such as halomethanes and ammonium salts, or even the xenon atom in organic solution. This gaseous guest occupies a special place due to its important role in biomedical applications and magnetic resonance imaging.[2] Besides their interesting binding properties, cryptophane derivatives are inherently chiral molecules and the presence of six aromatic rings interacting together inside a rigid molecular frame, by an excitonic coupling mechanism, makes the study of these systems by electronic circular dichroism (ECD) spectroscopy very attractive.[3] In addition, the enantiopure derivatives are expected to show a specific ECD response upon complexation, induced by a conformational change of the bridges of the cryptophane host. Additional parameters such as the nature of the solvent, which can compete with the guest molecule, are also expected to play a key role in the observed ECD effects.

Despite the interesting chiroptical properties of cryptophanes, only a very small number of papers have addressed this topic. This is mainly due to the difficulties for chemists to synthesize such materials in their enantiopure form in adequate amounts. Collet and co-workers were the first to report the synthesis of a series of enantio-enriched crypto-

[a] A. Bouchet, Dr. D. Cavagnat, Dr. T. Buffeteau
Institut des Sciences Moléculaires (CNRS - UMR5255)
Université Bordeaux 1, 351, Cours de la Libération
33405 Talence (France)
Fax: (+33) 540008402
E-mail: t.buffeteau@ism.u-bordeaux1.fr

[b] Dr. T. Brotin
Laboratoire de Chimie (CNRS - UMR5182)
Ecole Normale Supérieure de Lyon, 46 Allée d'Italie
69364 Lyon (France)
Fax: (+33) 472728860
E-mail: t.brotin@ens-lyon.fr

Supporting information for this article is available on the WWW under http://dx.doi.org/10.1002/chem.200902740.

phanes (90–95% *ee*) based on the resolution of enantiopure cyclotriveratrylene units.[3] Unfortunately, the small amount of material available prevented the complete investigation of the chiroptical properties of these host molecules as a function of the nature of the solvent or the presence (or not) of a guest inside the cavity. In 2003, Brotin and coworkers reported a novel approach, based on the optical resolution of cryptophane diastereomers, to provide the two enantiomers of cryptophane-A and its relatives in fair amounts.[4] This approach has been used with success to synthesize new enantiopure derivatives, the chiroptical properties of which have been determined by means of polarimetry as well as electronic and vibrational circular dichroism spectroscopic methods.

Vibrational circular dichroism (VCD) can provide more information than ECD can in the UV/Vis range. The VCD method measures the differential absorption of left versus right circularly polarized IR radiation for the $3N-6$ molecular vibration transitions, in which N is the number of atoms in the molecule.[5] Another advantage of VCD is reliable theoretical support. Quantum mechanical predictions of VCD spectra are quite successful in replicating the corresponding experimental spectra in the mid IR region.[5c] Ab initio calculations combined with VCD experiments have been used during the last two decades to determine the absolute configuration of small and medium-sized molecules[5b–d] and more recently to elucidate supramolecular structures.[6] Cryptophane molecules are small enough (100–150 atoms) to allow the use of ab initio calculations at the density functional theory (DFT) level, allowing the prediction of both the IR and VCD spectra of cryptophanes and their complexes for given conformations of the bridges. Thus, for the first time, we have been able to determine the absolute configuration of the two enantiomers of the cryptophane-A derivative and some of its congeners.[7] These studies also provided information about the conformation of the linkers. For instance, the presence of bulky guests, such as a chloroform molecule, inside the cavity of the host molecule strongly modifies the conformation of the linkers and leads to a preferential *all-trans* conformation, whereas the empty host adopts preferentially a *gauche* conformation of the bridges to reduce the volume of its inner cavity.[8] These VCD experiments as well as the more conventional ECD and polarimetry experiments have revealed that the solvent plays a key role in the chiroptical properties of these hosts, depending on the solvent's ability to enter the cavity or not.

However, very small spectral changes were observed in the IR and VCD spectra of cryptophane-A derivatives when the size of the guest molecule was changed (42, 56.3, and 72.2 Å^3 for xenon, dichloromethane, and chloroform, respectively). Moreover, the poor solubility of cryptophanes prevents us from investigating the chiroptical properties of these molecules in a large range of solvents, because a concentration of about 10^{-2} M is usually required for VCD experiments. For instance, these molecules are well soluble in [D_2]dichloromethane and [D]chloroform, sparingly soluble in 1,1,2,2-[D_2]tetrachloroethane, and unfortunately totally insoluble in water. Nevertheless, the synthesis of enantiopure water-soluble cryptophanes would be of great interest, because more pronounced chiroptical effects could be expected due to the hydrophobic character of the cryptophane host.

We report in this article the synthesis of the water-soluble cryptophanol **1** derivative. The chiroptical properties of its two enantiomers *MM*-**1** and *PP*-**1** in water were investigated under basic conditions (pH > 12) by polarimetry, electronic circular dichroism, and vibrational circular dichroism. The effects of the pH, the counterions, and the size of the guest molecules on the chiroptical properties of host **1** were studied. Finally, ab initio calculations at the density functional theory level were performed to interpret the chiroptical changes.

Results

Synthesis of resolved water-soluble cryptophanes: The synthetic route used to obtain water-soluble cryptophanol **1** from cryptophane-A **3** and monofunctionalized cryptophanol **2** derivatives is presented in Scheme 1. Racemic cryptophanol **2** was first prepared by a multistep synthesis from vanillin alcohol according to a procedure described by Darzac et al.[9] Chiral cryptophanol *MM*-**2** and *PP*-**2** derivatives were prepared from cryptophane diastereomers by reaction of *rac*-**2** with (−)-camphanic acid chloride according to a known procedure.[4] The separation of the two diastereomers by crystallization in toluene, followed by hydrolysis under basic conditions, yielded the desired cryptophanols **2** in their enantiopure forms (99–100%). This approach gives

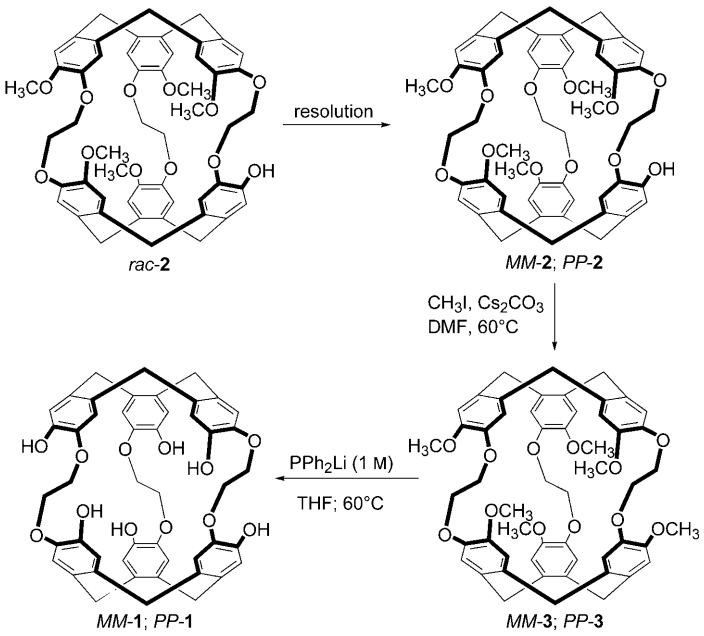

Scheme 1. Synthesis of enantiopure cryptophanols *MM*-**1** and *PP*-**1**.

the *MM*-**2** and *PP*-**2** derivatives in fair yield and provides a sizeable amount (0.1–0.5 g scale) of each enantiomer for subsequent reactions, taking advantage of the presence of the reactive hydroxyl group. Thus, the racemic cryptophane-A *rac*-**3** and its two enantiomers *MM*-**3** and *PP*-**3** were prepared by reaction of *rac*-**2**, *MM*-**2**, and *PP*-**2**, respectively, with methyl iodide in the presence of cesium carbonate in *N*,*N*-dimethylformamide (DMF) as previously reported.[4]

The following route was used for the synthesis of *rac*-**1** from *rac*-**3** (see Scheme 1): cryptophane-A (0.3 g, 0.34 mmol) was introduced into a 25 mL three-neck flask. Freshly distilled THF (4 mL) was then added and the suspension was stirred under argon at room temperature. A solution of lithium diphenylphosphide (PPh_2Li) in THF (≈1.0 M; 6 mL, 6 mmol) was added dropwise by syringe under an argon atmosphere (freshly prepared PPh_2Li is recommended for the reaction).[10] After complete addition of the PPh_2Li, the dark red solution was stirred overnight at 60 °C under argon. Then, the orange solution was poured into water; this resulted in a milky solution forming. The aqueous phase was extracted three times with CH_2Cl_2. Acidification of the aqueous phase with concentrated HCl led to the formation of a white precipitate, which was collected on a frit and successively washed with distillated water and diethyl ether. The solid was then purified on silica gel (short column, solvent DMF/acetone 50:50). After evaporation of the solvent under reduced pressure and digestion in diethyl ether, a white-beige precipitate was collected on a frit; this gave 0.2 g (74%) of a clean product. Enantiopure *MM*-**1** (70%) and *PP*-**1** (74%) derivatives were obtained by using the same experimental procedure. The nomenclature used to differentiate the two enantiomers of *rac*-**1**, *rac*-**2**, and *rac*-**3** is that suggested by Prof. V. Prelog for the specification of the absolute configuration of C_3-CTV derivatives in accordance with IUPAC rules.[11]

The *rac*-**1**, *MM*-**1**, and *PP*-**1** derivatives were found to be well soluble in DMSO, DMF, and water under basic conditions (pH > 12). ^{1}H NMR spectra of *rac*-**1**, *MM*-**1**, and *PP*-**1** are reported in the Supporting Information (Figure S1). These spectra recorded in NaOD or DMSO do not show any residual methoxy signals in the 3.5–4.0 ppm region. In addition, the NMR spectra recorded in NaOD solvent do not show any additional signals in the aromatic region that could reveal the presence of an "imploded" form of host **1**, as recently observed for another water-soluble cryptophane derivative.[1m] Thus, only two signals with the same intensity are observed, at 6.6 and 6.7 ppm, respectively, in good agreement with the D_3-symmetrical structure of **1** shown in Scheme 1. [**1**: Mp > 250 °C (decomp); ^{1}H NMR (500 MHz, [D$_6$]DMSO, 20 °C): $\delta = 8.58$ (s, 6H; OH), 6.62 (s, 6H; Ar), 6.58 (s, 6H; Ar), 4.40 (d, ^2J(H,H) = 13.4 Hz, 6H; H$_a$), 4.06 (m, 12H; OCH$_2$), 3.17 ppm (d, ^2J(H,H) = 13.4 Hz, 6H; H$_e$); ^{13}C NMR (125.6 MHz, [D$_6$]DMSO, 20 °C): $\delta = 146.4$ (6C), 144.4 (6C), 134.2 (6C), 130.1 (6C), 120.5 (6C), 117.7 (6C), 68.8 (6C; O*C*H$_2$), 35.0 ppm (6C; *C*H$_2$).]

Polarimetric measurements: Polarimetric measurements of empty *MM*-**1** and *MM*-**1** in the presence of CH_2Cl_2 and $CHCl_3$ in water were recorded under basic conditions, obtained by using aqueous solutions of LiOH, NaOH, KOH, and CsOH at an arbitrary concentration of 0.1 M. The optical rotation values are reported in Table 1 for several wavelengths and were completed by the values obtained in organic solvents (DMF, DMSO). As shown in Table 1, polarimetric measurements were found to be strongly dependent on the nature of the cations. Indeed, both the sign and the magnitude of the optical rotation values change drastically with the nature of the cations. For instance, the optical rotation values of empty *MM*-**1** at the sodium line ($[\alpha]_{589}$) are positive and have values of +10.4 and +0.8 for Li^+ and Na^+, respectively, whereas $[\alpha]_{589}$ values are negative and have values of −47.9 and −36.1 for K^+ and Cs^+, respectively. Even though the small positive value measured for the optical rotation in the case of Na^+ is questionable, because its magnitude lies in the range of the experimental error, a clearly positive value is measured in the case of Li^+. This is the first time that we have observed a reversal of the sign of the optical rotatory power for a cryptophane host by chang-

Table 1. Optical rotations $[\alpha]^{\lambda}_{25}$ [10^{-1} deg cm^2 g^{-1}] of *MM*-**1** and *PP*-**1** at 25 °C (experimental errors are estimated to be ±5%).

	Solvent	Conc [g/100 mL]	$[\alpha]^{589}_{25}$	$[\alpha]^{577}_{25}$	$[\alpha]^{546}_{25}$	$[\alpha]^{436}_{25}$
MM-**1**	DMF	0.16	−173.2	−183.4	−212.5	−409.8
PP-**1**	DMF	0.30	+175.0	+184.7	+215.1	+416.1
MM-**1**	DMSO	0.17	−84.3	−87.8	−102.0	−192.0
PP-**1**	DMSO	0.20	+83.2	+87.2	+97.5	+193.7
MM-**1**	D$_2$O/NaOH	0.20	+0.8[a]	+1.8[a]	+2.7[a]	−3.1[a]
PP-**1**	D$_2$O/NaOH	0.21	−1.4[a]	−1.3[a]	−1.3[a]	+3.8[a]
MM-**1**+CH_2Cl_2	D$_2$O/NaOH	0.19	−26.4	−27.6	−32.3	−47.3
PP-**1**+CH_2Cl_2	D$_2$O/NaOH	0.16	+24.1	+25.3	+29.0	+47.2
MM-**1**+$CHCl_3$	D$_2$O/NaOH	0.15	−44.4	−47.6	−53.0	−100.0
PP-**1**+$CHCl_3$	D$_2$O/NaOH	0.19	+42.3	+46.8	+53.8	+103.2
MM-**1**	D$_2$O/LiOH	0.18	+10.4	+10.6	+11.2	+22.9
MM-**1**+CH_2Cl_2	D$_2$O/LiOH	0.12	−28.4	−28.4	−30.4	−52.7
MM-**1**+$CHCl_3$	D$_2$O/LiOH	0.23	−33.7	−34.0	−39.0	−74.0
MM-**1**	D$_2$O/KOH	0.18	−47.9	−51.5	−60.6	−153.2
MM-**1**+CH_2Cl_2	D$_2$O/KOH	0.17	−45.3	−48.7	−59.1	−147.5
MM-**1**+$CHCl_3$	D$_2$O/KOH	0.19	−47.7	−51.9	−61.7	−153.1
MM-**1**	D$_2$O/CsOH	0.18	−36.1	−38.6	−46.7	−120.5
MM-**1**+CH_2Cl_2	D$_2$O/CsOH	0.17	−36.1	−37.6	−45.8	−117.2
MM-**1**+$CHCl_3$	D$_2$O/CsOH	0.25	−35.3	−37.3	−45.6	−117.9

[a] Optical rotation values with larger experimental errors.

ing the experimental conditions. As a consequence, the sign of the optical rotation values cannot be used to determine the absolute configuration of this water-soluble cryptophane derivative.

The optical rotation values were also found to be very sensitive to the presence of a guest molecule in the inner cavity of **1** for Li^+ and Na^+ ions. Indeed, a change of the sign and a significant increase of the optical rotatory power upon complexation were noticed with respect to the empty host. On the other hand, no significant changes of the optical rotation values were observed upon complexation for K^+ and Cs^+ ions. Finally, in organic solvents, the optical rotation values were much larger and were found to be strongly dependent on the nature of the solvent.

UV/Vis and ECD measurements: UV/Vis and ECD spectra of empty *MM*-**1** were recorded at 20 °C under basic conditions, by using aqueous solutions of LiOH, NaOH, KOH, and CsOH at an arbitrary concentration of 0.1 M. The UV/Vis spectra (220–360 nm spectral range) of empty *MM*-**1** and *MM*-**1** in the presence of CH_2Cl_2 and $CHCl_3$ are reported in the Supporting Information (Figure S2). The UV/Vis spectra exhibit a strong absorption band below 220 nm corresponding to the allowed ^1B_b transition (Platt's notation) of the benzene rings and two absorption bands of medium intensity around 240 and 300 nm corresponding to the two symmetry forbidden ^1L_a and ^1L_b transitions of the benzene rings, respectively. The ECD spectra of empty *MM*-**1** are reported in Figure 1 A in the same spectral range and show a significant change of the Cotton bands of the *MM*-**1** host according to the nature of the cation. For instance, similar ECD spectra are observed for Li^+ and Na^+, whereas the ECD spectra of *MM*-**1** undergo a bathochromic shift when K^+ and Cs^+ are used. In addition, a significant enhancement of the intensity of the Cotton bands associated with the ^1L_b transition (280–330 nm) occurs for the two latter cations. Additional experiments were performed with aqueous NaOH solution at different pH. As shown in Figure 1 B, the ECD spectra are also strongly pH dependent. Indeed, both the Cotton bands associated with the ^1B_b (<230 nm) and the ^1L_b (>280 nm) transitions are strongly affected by a change in pH, whereas the Cotton bands of the ^1L_a transition (240–260 nm) are less affected. For instance, at a NaOH concentration of 0.0015 M, the ECD spectrum contains two Cotton bands with opposite sign in the ^1L_b region and a positive Cotton band in the ^1B_b region. At higher concentration ([NaOH] = 1.0 M), there are two negative Cotton bands for the ^1L_b transition and a strong negative Cotton band for the ^1B_b transition.

A series of experiments were carried out to investigate the ability of a guest molecule to enter the cavity of **1**. All the experiments were performed in an aqueous NaOH solution at an arbitrary concentration of 0.1 M. Figure 2 shows the ECD spectra recorded for the empty or complexed (methane and chlorinated guests) *MM*-**1** enantiomer. Upon encapsulation, the ECD spectra reveal a significant change of the chiroptical properties of **1**, which depends on the size

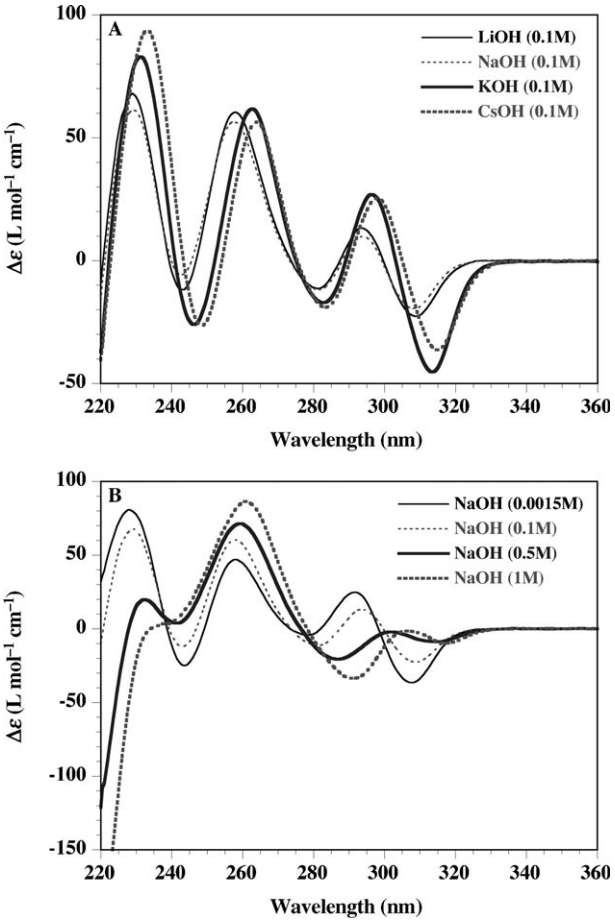

Figure 1. ECD spectra of *MM*-**1**: A) in solutions of LiOH, NaOH, KOH, and CsOH in H_2O (0.1 M), and B) in NaOH aqueous solution at different pH values.

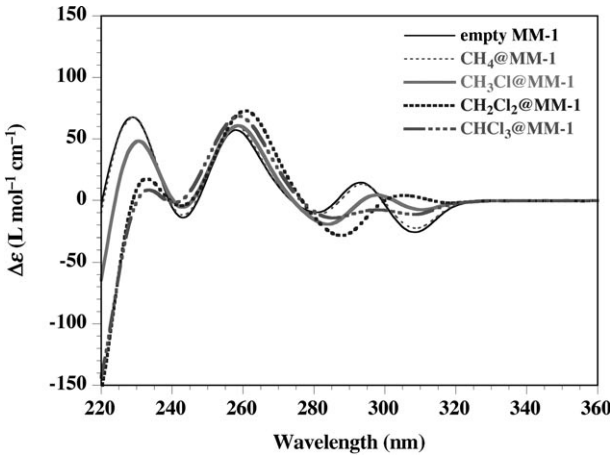

Figure 2. ECD spectra of *MM*-**1** in H_2O; an aqueous NaOH solution in the presence of different guests was used. The ECD spectrum of *MM*-**1** in the presence of CCl_4 (not shown) is identical to that of the empty *MM*-**1**.

of the guest. The most significant changes occur for the Cotton bands associated with the ^1B_b and ^1L_b transitions. Thus, specific ECD spectra were obtained for CH_3Cl@*MM*-**1**, CH_2Cl_2@*MM*-**1**, and $CHCl_3$@*MM*-**1** complexes. However,

when the guest molecule is too small (CH_4) or too bulky (CCl_4), the ECD spectrum is identical to that of the empty host **1**. Finally, as expected for two enantiomers, the ECD spectra of *MM*-**1** and *PP*-**1** show perfect mirror images, with the presence of an isosbestic point at 239 nm (see Supporting Information, Figure S3).

We also investigated the effect of the encapsulation as a function of the nature of the counterion. Thus, a new series of experiments were performed with Li^+, K^+, and Cs^+ as counterions and CH_2Cl_2 and $CHCl_3$ as guest molecules. The ECD spectra are reported in Figure 3 for aqueous solutions

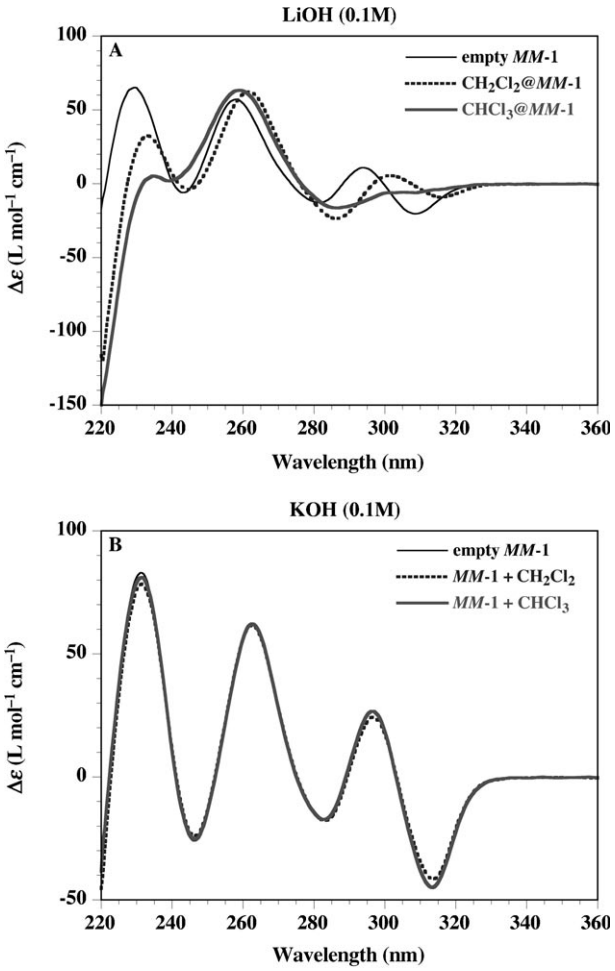

Figure 3. ECD spectra of empty *MM*-**1** as well as *MM*-**1** in the presence of CH_2Cl_2 and $CHCl_3$ in H_2O: aqueous solutions of A) LiOH and B) KOH were used.

of LiOH and KOH. Interestingly, very surprising host–guest behavior occurs depending on the counterion used. For instance, similar behavior is observed when Li^+ or Na^+ is used as counterion (Figure 3A) and the encapsulation of CH_2Cl_2 and $CHCl_3$ results in large changes in the ECD spectra of **1**. On the other hand, when K^+ is used as a counterion (Figure 3B), the ECD spectra of empty *MM*-**1** and *MM*-**1** in the presence of CH_2Cl_2 and $CHCl_3$ remain unchanged and no encapsulation effect is observed. Similar behavior was seen when Cs^+ was used as a counterion (see Supporting Information, Figure S4). It is remarkable that the nature of the counterion can have such an influence on the overall chiroptical properties of the host.

IR and VCD measurements: IR and VCD experiments were performed on samples in D_2O, with a host concentration of 0.030 M to provide VCD spectra with a sufficient signal-to-noise ratio. IR absorption spectra of *rac*-**1** were recorded under various basic conditions using solutions of NaOD in D_2O at different concentrations from 0.056 M (pD = 13.6) to 0.592 M (pD = 14.6). These extremely basic conditions are essential to dissolve cryptophanol **1** properly in D_2O at a concentration of 0.030 M. IR spectra of the 1450–1550 cm^{-1} spectral range, associated with the $\nu_{19a}C{=}C$ stretching vibration of the rings, for which the changes are the most noteworthy, are reported in Figure 4. There is a

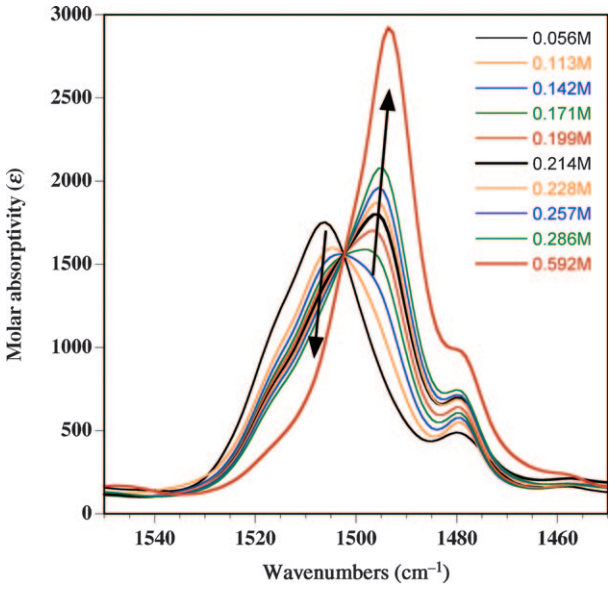

Figure 4. IR spectra of *rac*-**1** in D_2O; solutions of NaOD in D_2O at different concentrations were used. The concentration of host **1** was 0.030 M.

clear isobestic point at 1502 cm^{-1} between two main components. The respective proportions of the two components vary considerably according to the concentration of sodium. At low concentration of NaOD, only the high frequency component located at 1506 cm^{-1} is observed. When the concentration of sodium increases, the low-frequency component at 1495 cm^{-1} grows, while the high-frequency component collapses. At very high concentration of NaOD (0.59 M), only the low-frequency component is present. It is worth noting that the molar absorptivity of the low-frequency component is significantly higher than that of the high-frequency one. The same behavior occurred when Na^+ was replaced by Li^+, K^+, and Cs^+ ions (see Supporting Information, Figures S5 and S6).

The IR and VCD spectra of empty and complexed *PP*-**1** are reported in Figure 5. Samples in D_2O with 0.21 M NaOD

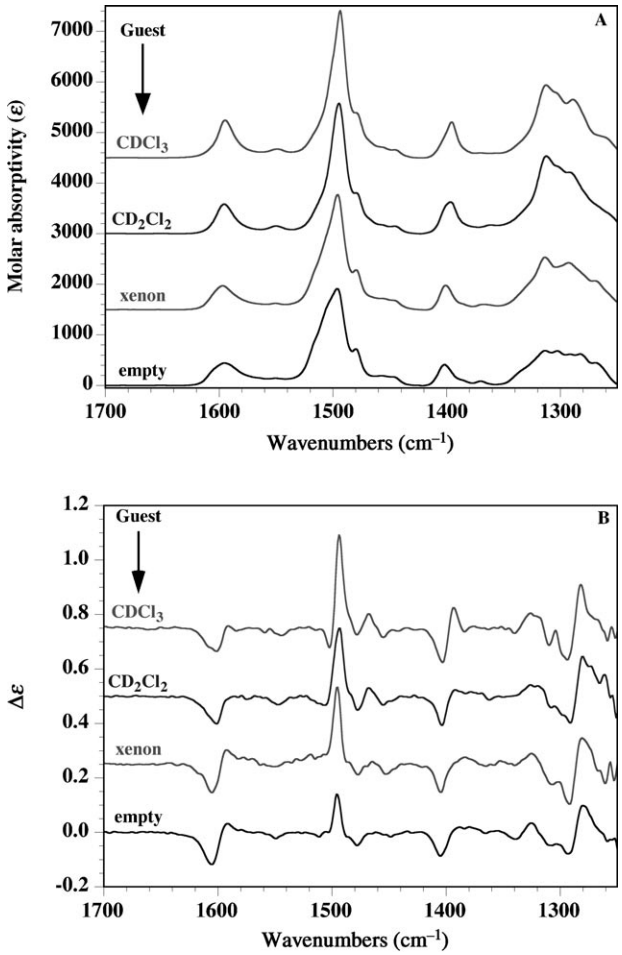

Figure 5. A) IR and B) VCD spectra of empty *PP*-**1** as well as Xe@*PP*-**1**, CD_2Cl_2@*PP*-**1**, and $CDCl_3$@*PP*-**1** complexes in D_2O; a solution of NaOD in D_2O (0.21 M) was used. The concentration of host **1** was 0.030 M.

were used. The spectra were recorded in the presence of various guest molecules (argon, xenon, CD_2Cl_2, $CDCl_3$, and CCl_4) and are presented in the 1700–1250 cm^{-1} region. The assignment of cryptophane-A derivatives in this spectral range has been reported previously.[7a] The bands due to the $\nu_{8a}C{=}C$ and $\nu_{19a}C{=}C$ stretching vibrations of the rings occur at 1595 and 1495 cm^{-1}, respectively. The bending vibrations of CH_2 groups give rise to the bands observed in the 1460–1440 cm^{-1} region. The band located at 1400 cm^{-1} and those observed between 1350 and 1250 cm^{-1} correspond to coupled modes involving wagging and twisting vibrations of the CH_2 groups (chains and bowls). As shown in Figure 5 A, when a guest molecule is encaged in the host **1**, most of the absorption bands sharpen and are enhanced. This effect, observed when xenon is present in solution, is more pronounced with CD_2Cl_2 molecules and even more with $CDCl_3$. This encapsulation effect is also clearly evidenced in the VCD spectra.

As shown in Figure 5 B, the bands located at 1495 cm^{-1} and in the 1350–1250 cm^{-1} spectral range are enhanced, and negative and positive components emerge at 1503 and 1393 cm^{-1}, respectively. It is worth noting that the presence of argon or CCl_4 in solution does not modify the IR and VCD spectra of the empty host **1** (spectra not shown). For a higher concentration in sodium (0.59 M), the same spectral changes occur in the VCD spectra, even for the empty cryptophane (see Supporting Information, Figure S7). In this case, there is no additional spectral change induced by the presence of the guest molecules. The behavior was similar when Li^+ was used as a counterion (see Supporting Information, Figure S8).

A new series of IR and VCD experiments was performed with solutions of deuterated potassium and cesium hydroxide in D_2O at a concentration of 0.21 M. As shown in Figure 6, the absorption (Figure 6 A) and VCD (Figure 6 B)

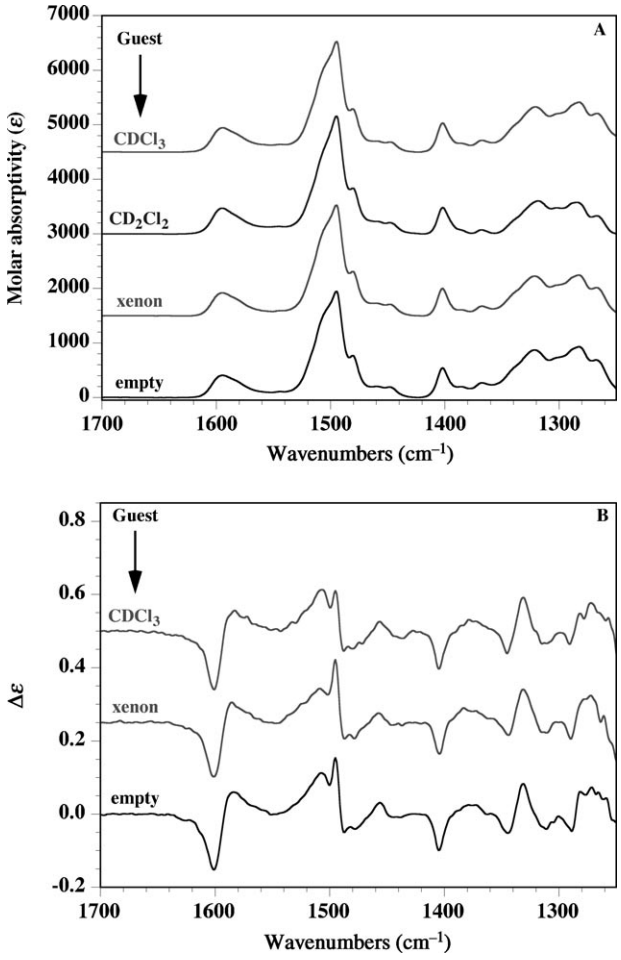

Figure 6. A) IR and B) VCD spectra of empty *PP*-**1** as well as *PP*-**1** in the presence of xenon, CD_2Cl_2 and $CDCl_3$ in D_2O; a solution of KOD in D_2O (0.21 M) was used. The concentration of host **1** was 0.030 M.

spectra did not change when any of the guest molecules was added to the solution. It seems that there is no interaction between the guest molecules and the cryptophane in KOD solution. However, it is noteworthy that the VCD spectrum of empty *PP*-**1** is different in the 1550–1480 cm^{-1} region from that of the NaOD solution. Indeed, the positive component at 1495 cm^{-1} appears in a dispersion profile shape.

For a higher concentration in potassium (0.59 M), as observed previously for the NaOD solution, spectral changes (i.e., enhancement of the bands located at 1495 cm^{-1} and in the 1350–1250 cm^{-1} spectral range as well as the emergence of a negative and positive components at 1503 and 1393 cm^{-1}, respectively) occur both in the presence and in the absence of a guest molecule in the cavity (see Supporting Information, Figure S9). The behavior was similar when Cs^+ was used as counterion (see Supporting Information, Figure S10).

Discussion

pH effect: The IR experiments performed on *rac*-**1** at different concentrations of NaOD (i.e., different pD) reveal the presence of two components responsible for the absorption bands associated with the νC=C stretching vibration of the benzene rings. Thus, for the ν_{19a}C=C stretching vibration of the rings close to 1500 cm^{-1}, the two components appear at 1506 and 1495 cm^{-1} and their intensities respond oppositely as a function of the concentration of sodium (see Figure 4). The presence of an isosbestic point suggests that there is an equilibrium between the two different forms of cryptophanol **1**. Since the concentration of cryptophanol (i.e., 0.030 M) is not significantly lower than that of the sodium deuterated hydroxide, we believe that cryptophanol is not totally deprotonated and consequently the phenol form of the molecule coexists with the phenolate form. To confirm this hypothesis, DFT calculations of the IR spectra were carried out for the phenol and phenolate forms of the molecule.

The calculated IR spectra at the B3PW91/6-31G* level for the $t_1t_1t_1$ conformers of both the phenol (6OD) and phenolate (6ONa) forms of *PP*-**1** are reported in Figure 7 and are compared with the experimental IR spectrum of empty *PP*-**1** in D_2O with NaOD solution (0.21 M). The calculated IR spectra of the phenol and phenolate forms of *PP*-**1** are rather different, confirming that the IR spectrum is strongly affected by the state of ionization of the hydroxyl groups. Concerning the ν_{19a}C=C stretching vibration close to 1500 cm^{-1}, the frequency calculated for the phenolate form is 10 cm^{-1} lower than that calculated for the phenol form, and its intensity is about twice as high. This result confirms the spectral changes observed in the IR spectra recorded at higher concentrations of sodium. It is clear that the low frequency component of the ν_{19a}C=C stretching mode is characteristic of the deprotonated phenolate form whereas the high frequency component is characteristic of the phenol form of the cryptophanol **1**. As shown in Figure 7, the half-sum of the two calculated spectra (labeled "3OD + 3ONa") reproduces the experimental spectrum recorded for a 0.21 M sodium concentration fairly well. This result indicates that a half of the hydroxyl groups are deprotonated when the sodium concentration is seven times higher than that of the cryptophanol. On the other hand, for the highest sodium concentration (i.e., 0.59 M), all the hydroxyl groups are deprotonated. This pH effect must be taken into account to correctly analyze the IR and VCD experiments under basic conditions.

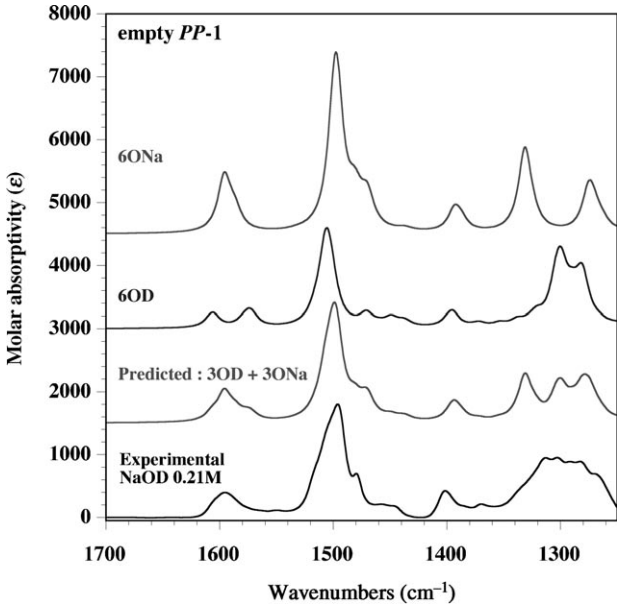

Figure 7. Comparison of the experimental IR spectrum of empty *PP*-**1** in D_2O when a solution of NaOD in D_2O (0.21 M) was used with the calculated spectra at the B3PW91/6-31G* level for $t_1t_1t_1$ conformers of the phenol (6OD) and phenolate (6ONa) forms of *PP*-**1**. The half-sum of the two predicted spectra is also reported (labeled 3OD + 3ONa).

For ECD experiments, it is clear that all the hydroxyl groups are deprotonated, because the concentration of cryptophanol is one thousand times smaller than that of the sodium cations present in solution.

Encapsulation effect: In previous studies, we showed that VCD and ECD spectra of enantiopure cryptophane A had very little dependence on the ability of a guest molecule to enter the cavity of these derivatives or not.[7a,b] Indeed, experiments performed in CD_2Cl_2, $CDCl_3$, and $C_2D_2Cl_4$ (a molecule which cannot enter the cryptophane-A cavity) reveal no significant differences in the IR and VCD spectra.[7a] Similarly, the ECD spectra recorded of samples in $CHCl_3$ and CH_2Cl_2 (two solvents that enter the cavity of cryptophane-A) and of samples in CH_3CN and THF (two solvents that do not enter the cavity of cryptophane-A) were quasi-identical, even if small spectral changes were observed in the 260–310 nm region, associated with the ^1L_b transition.[7b] The solvent effect was found more pronounced for cryptophane-A with C_1 symmetry, in particular for cryptophane-A monofunctionalized with an electron-withdrawing triflic moiety or a hydrogen atom.[7b,c] This effect was attributed to a change of conformation of the linkers upon encapsulation.

The ECD and VCD chiroptical changes upon encapsulation are significantly more marked when cryptophanol **1** is dissolved in water under basic conditions. This was the first time since we had started studying chiroptical properties of cryptophanes that such spectral differences in both VCD

and ECD spectra were observed. It seems reasonable to interpret the chiroptical changes in the following way. Empty host **1**, which is a lipophilic molecule, even though it is soluble under basic conditions (pH $\geq$12), adopts a preferential *gauche* conformation of the linkers to reduce the size of its internal cavity in water. In contrast, upon encapsulation, the presence of a guest molecule inside its cavity requires host **1** to change the conformation of its linkers to enlarge its cavity and to accommodate a guest molecule. Thus, upon encapsulation, host **1** adopts preferentially a *trans* conformation of the linkers when large molecules are present in the cavity of **1**. This was previously demonstrated for cryptophane-A derivatives soluble in organic solvents.[7b,c] Of course the change of conformation strongly depends on the size of the guest. A large guest such as a chloroform molecule (van der Waals volume, $V_{vdw}=72.2$ Å^3)[12] is less easily accommodated in the cavity of **1** compared to a dichloromethane guest ($V_{vdw}=56.3$ Å^3) and thus it requires host **1** to significantly enlarge the size of its cavity.

To confirm that a conformational change of the linkers can explain the VCD spectral changes, DFT calculations of the VCD spectra of empty *PP*-**1** and the $CDCl_3$@*PP*-**1** complex were carried out for both the phenol and phenolate forms of the molecule. For each form, the calculations were performed for *all-gauche* ($g_1g_1g_1$) and *all-trans* ($t_1t_1t_1$) conformations of the three linkers. By using starting O-C-C-O dihedral angles close to 180° and −60° for the t_1 and g_1 conformations, respectively, the geometries of the empty and complexed cavities were optimized at the B3PW91/6-31G* level. Harmonic vibrational frequencies were calculated at the same level to confirm that all structures are stable conformations and to enable free energies to be calculated. The converged twist angles between the two CTV bowls, O-C-C-O dihedral angles, and optimized energies are listed in Table 2. The optimized geometries of empty *PP*-**1** calculated for the two conformations lead to very close Gibbs free energies for both phenol (6OD) and phenolate (6ONa) forms. Nevertheless, the $g_1g_1g_1$ conformation is more favorable for the deprotonated form of the cryptophanol. On the other hand, for $CDCl_3$@*PP*-**1**, the $t_1t_1t_1$ conformation of the aliphatic linkers yields a final optimized structure of the complex 4.3 kcal mol^{-1} lower in energy than the $g_1g_1g_1$ conformation. In addition, no convergence of the optimized geometries of the $g_1g_1g_1$ conformer was obtained for the phenolate form. The addition of a chloroform molecule in the cryptophanol cage stabilizes the $t_1t_1t_1$ conformer. A similar result was previously reported for cryptophane-A monofunctionalized with a hydrogen atom.[7c] This result is not surprising, because there is a better size match between the chloroform (ca. 72.2 Å^3) and the cryptophane cavity in its *all-trans* conformation (ca. 95 Å^3).

Table 2. Conformations and energies of *PP*-**1**.

Form	Conf.	Optimized geometries D[c] [°]	T[d] [°]	Energy[a] Electronic	Gibbs	ΔE[b]
empty *PP*-**1**						
6OD	$t_1t_1t_1$	169.1	37.0	−2755.932758	−2755.212639	0.0
	$g_1g_1g_1$	−63.9	41.7	−2755.935483	−2755.212229	0.26
6ONa	$t_1t_1t_1$	−172.0	73.3	−3726.306559	−3725.628896	0.41
	$g_1g_1g_1$	−55.9	46.1	−3726.301043	−3725.629542	0.0
$CDCl_3$@*PP*-**1**						
6OD	$t_1t_1t_1$	168.1	34.7	−4175.032763	−4174.303932	0.0
	$g_1g_1g_1$	−69.2	37.6	−4175.028620	−4174.297122	4.3
6ONa	$t_1t_1t_1$	−165.6	71.1	−5145.388530	−5144.701656	0.0
	$g_1g_1g_1$	no convergence				

[a] In Hartrees. [b] Relative Gibbs energy difference in kcal mol^{-1}. [c] Dihedral angle O-C-C-O. [d] Twist angle between the 2 CTV units.

The VCD spectra calculated at the B3PW91/6-31G* level for the $t_1t_1t_1$ and $g_1g_1g_1$ conformers of the phenol and phenolate forms of empty *PP*-**1** are reported in Figure 8 A. The predicted spectra were calculated for each form, taking into account the Gibbs free energies of the two conformers. Finally, the half-sum of the two predicted spectra of each form was calculated for comparison with the experimental VCD spectrum of empty *PP*-**1** recorded in D_2O using a sodium concentration of 0.21 M (see pH effect). Similarly, the half-

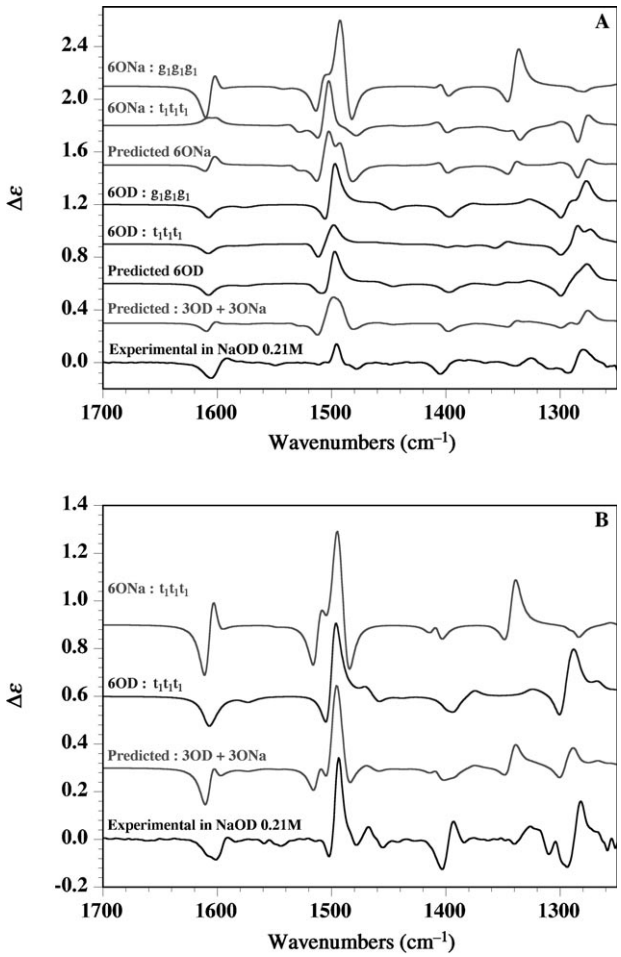

Figure 8. Comparison of the experimental VCD spectra of A) empty *PP*-**1** and B) $CDCl_3$@*PP*-**1** complex in D_2O when using a solution of NaOD in D_2O (0.21 M) with calculated spectra at the B3PW91/6-31G* level for $t_1t_1t_1$ and $g_1g_1g_1$ conformers of the phenol (6OD) and phenolate (6ONa) forms of *PP*-**1**. The half-sum of the two predicted spectra of 6OD and 6ONa is also reported (labeled 3OD + 3ONa).

sum of the VCD spectra calculated for the $t_1t_1t_1$ conformer of the phenol and phenolate form was compared to the experimental VCD spectrum of $CDCl_3$@*PP*-**1** complex (see Figure 8B). The spectral changes observed in the experimental spectra upon encapsulation are fairly well reproduced in the predicted VCD spectra, showing that a conformational change of the linkers is certainly at the source of this effect.

The size of the guest molecule plays a key role in the overall chiroptical properties of water-soluble cryptophanes. Specific ECD spectra of *MM*-**1** were obtained when chloromethane ($V_{vdw}=42$ Å^3), dichloromethane ($V_{vdw}=56.3$ Å^3), and chloroform ($V_{vdw}=72.2$ Å^3) were used as guest molecules, whereas methane ($V_{vdw}=24$ Å^3) and tetrachloromethane ($V_{vdw}=86.7$ Å^3) led to ECD spectra similar to that of empty *MM*-**1** (see Figure 2). The tetrachloromethane molecule is too large to be easily accommodated by host **1** and consequently cannot modify its chiroptical properties. Similar behavior was observed with the cryptophane-A congener. In contrast, methane easily enters the cavity of **1**, but its volume is too small to interact strongly with **1**, thus leaving the conformation of the bridges unchanged.

Other guest molecules such as CH_2BrCl ($V_{vdw}=60.4$ Å^3), CH_2Br_2 ($V_{vdw}=64.4$ Å^3), and CH_3I ($V_{vdw}=54.6$ Å^3) are also well recognized by *MM*-**1** and the ECD spectra of these complexes differ from each other (see Figure 9A). Thus, host **1** selectively recognizes each encapsulated species, even if there is a small difference in size between these three guests. In contrast, the ECD spectrum of *MM*-**1** with CH_2I_2 ($V_{vdw}=76.5$ Å^3) is perfectly identical (at least in the ^1L_b spectral region) to that of the empty host, suggesting that this guest is too large to enter the cavity of **1**. The ability of the ECD spectroscopy to discriminate supramolecular complexes of **1** with small neutral molecules is a remarkable characteristic of this host and it could find applications for the detection of chlorinated solvents dissolved in water. This encapsulation effect is essentially governed by the size of the guest molecules in water, but seems not dependent on the nature of the guest. Indeed, as shown in Figure 9B, similar ECD spectra were recorded when chloromethane or xenon were introduced into the solution. These two gases are interesting guest molecules because they have the same volume ($V_{vdw}=42$ Å^3), but different chemical properties.

It is worth noting that a change in the pH conditions produces similar effects on the ECD spectra (see Figure 1B) as that produced by the presence of a guest molecule inside the cavity of **1**. Thus, an increase of the concentration of cations certainly favors a preferential *trans* conformation of the linkers. Finally, the high selectivity of water-soluble cryptophane for guest molecules is related to the presence of the phenolate form of the two CTV units, which enhances the chiroptical properties of host **1** (the deviation of the electronic transition moment ^1L_b and ^1B_b induced by the phenolate moiety is larger than that induced by the phenol group).

Counterion effect: The counterion also plays a key role in the overall chiroptical properties of water-soluble cryptophanes. Two distinct effects were observed upon encapsulation depending on the size of the counterions. For Li^+ ($V=1.8$ Å^3) and Na^+ ($V=4.4$ Å^3) cations,[13] the encapsulation of CH_2Cl_2 and $CHCl_3$ results in large changes in the ECD and VCD spectra of **1**, whereas for K^+ ($V=11.0$ Å^3) and Cs^+ ($V=19.5$ Å^3) no encapsulation effect was observed: the ECD and VCD spectra as well as the optical rotation values remained unchanged compared to the empty cryptophanol **1**. Many allosteric effects upon encapsulation have been reported in the literature,[14] but to our knowledge this is the first time that changing the nature of the alkali metal cation induces such large changes in both the ECD and VCD spectra of a host molecule. In our opinion, this surprising behavior can be more easily interpreted by steric effects than by electronic effects. Indeed, host **1** and its congeners are inherently chiral molecules composed of two cyclotriveratrylene units connected by three ethylenedioxy bridges. This structure generates a lipophilic cavity ($V\approx95$ Å^3) suitable for the encapsulation of small guest molecules. Before entering the cavity, the guest molecule must cross one of the three portals to access the inner cavity of **1**. Under basic conditions, the size of the counterions surrounding the host molecule may prevent the guest molecule from reaching the cavity.

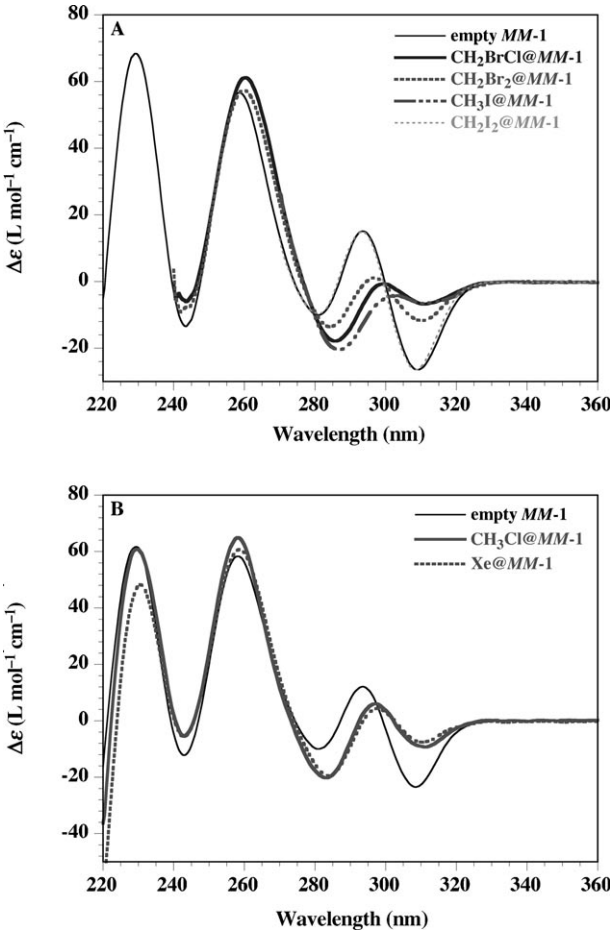

Figure 9. ECD spectra of *MM*-**1** in H_2O when using an aqueous NaOH solution in the presence of different guests.

Our results demonstrate that the potassium and cesium cations are large enough to prevent CH_2Cl_2 and $CHCl_3$ from entering the cavity of **1**. In contrast, the size of the lithium and sodium cations, significantly smaller, is not sufficient to obstruct the portals and allows guest molecules to enter the cavity of **1**. This assumption can be supported by examination of the optimized structures of *PP*-**1** for the phenolate form when using sodium and cesium cations. As shown in Figure 10, even if the six sodium cations are placed in front of the portals of **1**, they allow the entrance of $CDCl_3$ molecules. On the other hand, for bulky cations (cesium), the access to the cavity is impossible and no encapsulation effect can be observed. Counterions appear as an external factor, which can modify the chiroptical properties of the host by controlling the access of the guest to the inner cavity of **1**.

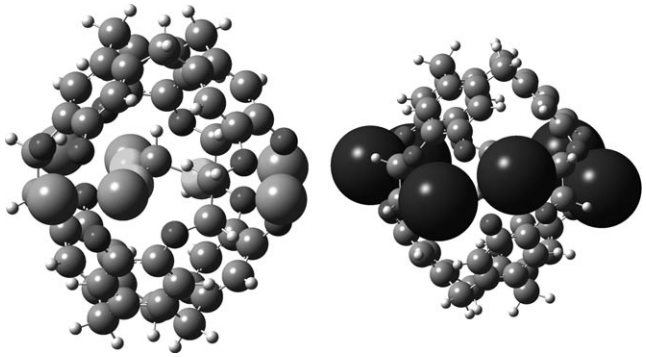

Figure 10. B3PW91/6-31G*-optimized structures of *PP*-**1** for the phenolate form when using sodium (left) and cesium (right) cations.

Similar behavior occurs in methanol, which shows no encapsulation effect on the ECD spectra of *MM*-**1** in the presence of CH_2Cl_2 or $CHCl_3$ (see Supporting Information, Figure S11). Steric congestion of the host surrounded by methanol molecules can also explain this feature. Indeed, methanol molecules can strongly interact with phenol groups by hydrogen-bonding interactions. Since the methanol molecules are unable to enter the cavity of cryptophane molecules, they stay at the periphery, close to the three portals of the host. Thus, methanol molecules ($V_{vdw}=36.1$ Å^3)[12] play a role similar to that of potassium and cesium cations by preventing guest molecules from reaching the inner cavity of **1**.

^{1}H NMR and UV/visible spectroscopy performed on *rac*-**1** nicely confirm these results. For instance, the ^{1}H NMR spectra (see Supporting Information, Figure S12) of empty *rac*-**1**, CH_2Cl_2@*rac*-**1**, and $CHCl_3$@*rac*-**1** show a clear difference in the NMR signals for the bridges ($\delta=4.7$–3.8 ppm region); this supports the concept of a change of conformation of the linkers upon encapsulation, which also depends on the nature of the guest molecule. In addition, for the CH_2Cl_2@*rac*-**1** complex in NaOD solution, a bound signal is clearly visible around 1.0 ppm, which is characteristic of a high-field-shifted signal due to the shielding effect of the six aromatic rings. In contrast, in KOD solution, no bound signal is detected under similar conditions, reflecting the absence of complex formation. UV/Vis spectroscopy of *rac*-**1** performed under different conditions (see Supporting Information, Figure S2) is also consistent with the overall ECD and VCD experiments. For instance, for LiOH and NaOH solutions, both CH_2Cl_2@*rac*-**1** and $CHCl_3$@*rac*-**1** show slightly different UV/Vis spectra compared to that of the empty *rac*-**1**, as a consequence of the encapsulation process. In contrast, for KOH and CsOH solutions, UV/Vis spectra are strictly identical, which is consistent with the absence of encapsulation under these conditions.

Conclusion

The two enantiomers of cryptophanol **1** were synthesized, and their chiroptical properties in water under basic conditions (pH > 12) were examined by polarimetry as well as ECD and VCD spectroscopy. The ECD and VCD experiments were performed by varying some parameters such as the nature of the counterion, the size of the guest molecule, and the pH conditions. Our results reveal unique behavior of host **1**, never observed with cryptophane-A and its relatives in organic solvents before. We showed that both the ECD and VCD spectra of **1** are extremely sensitive to external parameters such as the nature of the counterion (alkali metal Li^+, Na^+, K^+, and Cs^+) and the pH of the solution. Polarimetric measurements also reveal a change of the sign of the optical rotation values with respect to the used counterions. As a consequence, the determination of the absolute configuration of water-soluble cryptophanes should be examined with great caution, and the use of several chiroptical techniques (ECD, VCD) are thus recommended to ascertain the absolute configurations of these molecules. The aqueous solvent used under basic conditions seems to play a key role in the observed effect. Indeed, the antagonism between cryptophane (lipophilic molecule) and water induces a contraction of the host, which preferentially adopts a *gauche* conformation of the linkers to reduce the size of its internal cavity. Moreover, the presence of six phenolate moieties under basic conditions amplifies the chiroptical properties (ECD) of **1**, because they induce a larger deviation of the angle for both the ^1B_b, ^1L_a, and ^1L_b transition moments compared to the protonated species (experiments in methanol). The ECD and VCD experiments have shown the importance of the nature of the cation on the overall chiroptical properties of **1**. This surprising counterion effect can be more easily interpreted on the basis of steric effects. Small cations such as Li^+ or Na^+ are not bulky enough to obstruct the three portals of the host **1** and thus allow the guest molecules to enter the cavity of **1**. In turn, these guest molecules induce a conformational change, allowing the cryptophane to adopt an *all-trans* conformation of the linkers. As the size of the guest increases, the host **1** adopts a conformation of the linkers that enhances the size of its internal cavity (*trans* conformation) to accommodate the guest more easily. In contrast, the empty cryptophane in aqueous solution tends

to reduce its internal volume and preferentially adopts a *gauche* conformation of the linkers. Different behavior occurs for the K^+ and Cs^+ ions. Indeed, these two cations seem large enough to obstruct the portals of **1** and to prevent any guest from entering the cavity of the host. As a consequence, the chiroptical properties of the host remain unchanged. To our knowledge, this is the first time that such a counterion effect has been reported for a chiral host molecule. In addition, chiroptical properties of *MM*-**1** (in particular the ECD spectra) are strongly affected by the encapsulation of a guest molecule present inside the cavity, giving specific ECD spectra for various sizes of the guest molecules. This makes **1** a good sensor for the detection of small neutral molecules dissolved in water, and such a system could find application in environmental science.

Experimental Section

Polarimetric measurements: Optical rotations of *MM*-**1** and *PP*-**1** were measured at several wavelengths on a Jasco P-1010 polarimeter with a 100 mm cell thermostated at 25 °C.

UV/Vis and ECD measurements: UV/Vis and ECD spectra were recorded on Jasco V-550 and Chirascan spectrophotometers, respectively, at room temperature, and by using a 0.2 cm path length quartz cell (Hellma). The concentration of cryptophanol **1** was in the range of 5×10^{-5} to 10^{-4} M in basic H_2O solutions (0.1 M solutions of LiOH, NaOH, KOH, and CsOH). Spectra were recorded in the 220–450 nm wavelength range with a 0.5 nm increment and a 1 s integration time. Spectra were processed with Chirascan software, baseline-corrected, and slightly smoothed by using a third-order least-square polynomial fit. Spectral units were expressed in molar ellipticity.

IR and VCD measurements: The IR and VCD spectra were recorded on a ThermoNicolet Nexus 670 FTIR spectrometer equipped with a VCD optical bench.[15] IR absorption and VCD spectra were recorded at a resolution of 4 cm^{-1}, by co-adding 50 scans and 24000 scans (8 h acquisition time), respectively. Samples were contained in a CaF_2 cell with a fixed path length of 45 μm (BioCell™, BioTools). IR and VCD spectra were obtained of *MM*-**1** and *PP*-**1** in basic D_2O solutions (0.21 M and 0.59 M solutions of LiOD, NaOD, KOD, and CsOD) at a concentration of 0.030 M. Additional IR spectra of *rac*-**1** were recorded for various concentrations of LiOD, NaOD, KOD, and CsOD. Baseline corrections of the VCD spectra were performed by subtracting the two opposite-enantiomer VCD spectra of **1** (recorded under the same experimental conditions) with division by two. In all experiments, the photoelastic modulator was adjusted for a maximum efficiency at 1400 cm^{-1}. Calculations were carried out with the standard ThermoNicolet software, using Happ and Genzel apodization, de-Haseth phase-correction, and a zero-filling factor of one. Calibration spectra were recorded using a birefringent plate (CdSe) and a second BaF_2 wire grid polarizer, following the experimental procedure previously published.[16] Finally, in the presented IR spectra, the solvent absorption was subtracted out.

DFT calculations: The geometry optimizations, vibrational frequencies, absorption, and VCD intensities were calculated by the Gaussian 03 program[17] on the CIS-IBM (with sixteen processors) at the M3PEC computing center of the University Bordeaux I. Calculations of the optimized geometry of *PP*-**1** were performed at the DFT level using the B3PW91 functional and 6-31G* basis set. The theoretical framework for geometry optimization of cryptophane molecules has been published previously.[7a] Since IR and VCD spectra were recorded of basic D_2O solutions leading to partially deprotonated cryptophanol, DFT calculations were performed by considering the phenol (OD peripheral substituents) and phenolate (O^-Na^+ peripheral substituents) forms of the molecule. In a first step, we performed DFT calculations for the empty *PP*-**1**. The three $-OCH_2CH_2O-$ bridges were considered either with an *anti* conformation (referring to the bonds to the O atoms having a 180° dihedral angle, labeled $t_1t_1t_1$) or with a *gauche* conformation (−60° dihedral angle, labeled $g_1g_1g_1$). In a second step, geometry optimizations were performed by introducing a chloroform molecule inside the cryptophanol cavity, considering either a t_1 or g_1 conformation for the three ethoxy linkers ($t_1t_1t_1$ and $g_1g_1g_1$ conformers). Vibrational frequencies, IR, and VCD intensities were calculated at the same level of theory, utilizing the magnetic field perturbation method with gauge-invariant atomic orbitals.[18] For comparison to experiment, the calculated frequencies were scaled by 0.968 and the calculated intensities were converted into Lorentzian bands with a half-width of 7 cm^{-1}.

Acknowledgements

The authors are indebted to the CNRS (Chemistry Department) and to Région Aquitaine for financial support for FTIR and optical equipment. They also acknowledge computational facilities provided by the Pôle Modélisation of the Institut des Sciences Moléculaires and the M3PEC-Mésocentre of the University Bordeaux 1 (http://www.m3pec.u-bordeaux1.fr), financed by the Conseil Régional d'Aquitaine and the French Ministry of Research and Technology.

[1] a) A. Collet in *Comprehensive Supramolecular Chemistry, Vol. 2* (Eds.: J. L. Atwood, J. E. D. Davis, D. D. MacNicol, F. Vögtle), Pergamon Press, New York, **1996**, Chapter 11, pp. 325–365; b) T. Brotin, J. P. Dutasta, *Chem. Rev.* **2009**, *109*, 88–130; c) J. Canceill, M. Cesario, A. Collet, J. Guilhem, L. Lacombe, B. Lozach, C. Pascard, *Angew. Chem.* **1989**, *101*, 1249–1251; *Angew. Chem. Int. Ed. Engl.* **1989**, *28*, 1246–1248; d) L. Garel, J. P. Dutasta, A. Collet, *Angew. Chem.* **1993**, *105*, 1249–1251; *Angew. Chem. Int. Ed. Engl.* **1993**, *32*, 1169–1171; e) K. Bartik, M. Luhmer, J. P. Dutasta, A. Collet, J. Reisse, *J. Am. Chem. Soc.* **1998**, *120*, 784–791; f) M. Luhmer, B. M. Goodson, Y. Q. Song, D. D. Laws, L. Kaiser, M. C. Cyrier, A. Pines, *J. Am. Chem. Soc.* **1999**, *121*, 3502–3512; g) T. Brotin, A. Lesage, L. Emsley, A. Collet, *J. Am. Chem. Soc.* **2000**, *122*, 1171–1174; h) T. Brotin, T. Devic, A. Lesage, L. Emsley, A. Collet, *Chem. Eur. J.* **2001**, *7*, 1561–1573; i) J. Lang, J. J. Dechter, M. Effemey, J. Kowalewski, *J. Am. Chem. Soc.* **2001**, *123*, 7852–7858; j) Z. Tosner, J. Lang, D. Sandström, O. Petrov, J. Kowalewski, *J. Phys. Chem. A* **2002**, *106*, 8870–8875; k) T. Brotin, J. P. Dutasta, *Eur. J. Org. Chem.* **2003**, 973–984; l) J. G. Huber, L. Dubois, H. Desvaux, J. P. Dutasta, T. Brotin, P. Berthault, *J. Phys. Chem. A* **2004**, *108*, 9608–9615; m) J. G. Huber, T. Brotin, L. Dubois, H. Desvaux, J. P. Dutasta, P. Berthault, *J. Am. Chem. Soc.* **2006**, *128*, 6239–6246; n) H. A. Fogarty, P. Berthault, T. Brotin, G. Huber, H. Desvaux, J. P. Dutasta, *J. Am. Chem. Soc.* **2007**, *129*, 10332–10333; o) C. Zhang, W. Shen, G. Wen, J. Chao, L. Qin, S. Shuang, C. Dong, M. M. F. Choi, *Talanta* **2008**, *76*, 235–240.

[2] a) B. M. Goodson, *J. Magn. Reson.* **2002**, *155*, 157–216; b) A. Cherubini, A. Bifone, *Prog. Nucl. Magn. Reson. Spectrosc.* **2003**, *42*, 1–30; c) A. M. Oros, N. J. Shah, *Phys. Med. Biol.* **2004**, *49*, R105–R153; d) P. Berthault, A. Bogaert-Buchmann, H. Desvaux, G. Huber, Y. Boulard, *J. Am. Chem. Soc.* **2008**, *130*, 16456–16457.

[3] J. Canceill, A. Collet, G. Gottarelli, P. Palmieri, *J. Am. Chem. Soc.* **1987**, *109*, 6454–6464.

[4] T. Brotin, R. Barbe, M. Darzac, J. P. Dutasta, *Chem. Eur. J.* **2003**, *9*, 5784–5792.

[5] a) L. A. Nafie, R. K. Dukor, T. B. Freedman in *Handbook of Vibrational Spectroscopy, Vol. 1* (Eds.: J. M. Chalmers, P. R. Griffiths), Wiley, New York, **2002**, pp. 731–744; b) T. B. Freedman, X. Cao, R. K. Dukor, L. A. Nafie, *Chirality* **2003**, *15*, 743–758; c) P. J. Stephens, F. J. Devlin, *Chirality* **2000**, *12*, 172–179; d) P. J. Stephens, F. J. Devlin, J. J. Pan, *Chirality* **2008**, *20*, 643–663.

[6] a) F. Wang, P. L. Polavarapu, F. Lebon, G. Longhi, S. Abbate, M. Catellani, *J. Phys. Chem. A* **2002**, *106*, 5918–5923; b) V. Setnicka,

M. Urbanova, S. Pataridis, V. Kral, K. Volka, *Tetrahedron: Asymmetry* **2002**, *13*, 2661–2666; c) T. B. Freedman, X. Cao, A. Rajca, H. Wang, L. A. Nafie, *J. Phys. Chem. A* **2003**, *107*, 7692–7696; d) T. Bürgi, A. Urakawa, B. Behzadi, K. H. Ernst, A. Baiker, *New J. Chem.* **2004**, *28*, 332–334; e) M. Urbanova, V. Setnicka, F. J. Delvin, P. J. Stephens, *J. Am. Chem. Soc.* **2005**, *127*, 6700–6711; f) V. Setnicka, M. Urbanova, K. Volka, S. Nampally, J. M. Lehn, *Chem. Eur. J.* **2006**, *12*, 8735–8743; g) T. Buffeteau, L. Ducasse, L. Poniman, N. Delsuc, I. Huc, *Chem. Commun.* **2006**, 2714–2716; h) L. Ducasse, F. Castet, A. Fritsch, I. Huc, T. Buffeteau, *J. Phys. Chem. A* **2007**, *111*, 5092–5098; i) M. M. J. Smulders, T. Buffeteau, D. Cavagnat, M. Wolffs, A. P. H. J. Schenning, E. W. Meijer, *Chirality* **2008**, *20*, 1016–1022.

[7] a) T. Brotin, D. Cavagnat, J. P. Dutasta, T. Buffeteau, *J. Am. Chem. Soc.* **2006**, *128*, 5533–5540; b) D. Cavagnat, T. Buffeteau, T. Brotin, *J. Org. Chem.* **2008**, *73*, 66–75; c) T. Brotin, D. Cavagnat, T. Buffeteau, *J. Phys. Chem. A* **2008**, *112*, 8464–8470.

[8] The volume of the cryptophane-A cavity with its three spacer bridges in *gauche* and in *trans* conformations can be estimated at approximately 65 and 95 $Å^3$, respectively.

[9] a) M. Darzac, T. Brotin, D. Bouchu, J. P. Dutasta, *Chem. Commun.* **2002**, 48–49; b) M. Darzac, T. Brotin, L. Rousset-Azrel, D. Bouchu, J. P. Dutasta, *New J. Chem.* **2004**, *28*, 502–512.

[10] E. Vedejs, P. L. Fuchs, *J. Am. Chem. Soc.* **1973**, *95*, 822–825.

[11] a) *IUPAC 1968 Tentative Rules, Section E, Fundamental Stereochemistry* in *J. Org. Chem.* **1970**, *35*, 2849–2867; b) A. Collet, G. Gabard, J. Jacques, M. Césario, J. Guilhem, C. Pascard, *J. Chem. Soc., Perkin Trans. 1* **1981**, 1630–1638.

[12] Y. H. Zhao, M. H. Abraham, A. M. Zissimos, *J. Org. Chem.* **2003**, *68*, 7368–7373.

[13] The volumes of the alkali metal ions were calculated from their ionic radii.

[14] a) Y. Murakami, T. Ohno, O. Hayashida, Y. Hisaeda, *J. Chem. Soc. Chem. Commun.* **1991**, 950–952; b) G. A. Hembury, V. V. Borovkov, Y. Inoue, *Chem. Rev.* **2008**, *108*, 1–73, and references therein.

[15] T. Buffeteau, F. Lagugné-Labarthet, C. Sourrisseau, *Appl. Spectrosc.* **2005**, *59*, 732–745.

[16] L. A. Nafie, D. W. Vidrine in *Fourier Transform Infrared Spectroscopy, Vol. 3* (Eds.: J. R. Ferraro, L. J. Basile), Academic Press, New York, **1982**, pp. 83–123.

[17] Gaussian 03 (Revision B.04), M. J. Frisch, G. W. Trucks, H. B. Schlegel, G. E. Scuseria, M. A. Robb, J. R. Cheeseman, J. A. Montgomery Jr., T. Vreven, K. N. Kudin, J. C. Burant, J. M. Millam, S. S. Iyengar, J. Tomasi, V. Barone, B. Mennucci, M. Cossi, G. Scalmani, N. Rega, G. A. Petersson, H. Nakatsuji, M. Hada, M. Ehara, K. Toyota, R. Fukuda, J. Hasegawa, M. Ishida, T. Nakajima, Y. Honda, O. Kitao, H. Nakai, M. Klene, X. Li, J. E. Knox, H. P. Hratchian, J. B. Cross, C. Adamo, J. Jaramillo, R. Gomperts, R. E. Stratmann, O. Yazyev, A. J. Austin, R. Cammi, C. Pomelli, J. W. Ochterski, P. Y. Ayala, K. Morokuma, G. A. Voth, P. Salvador, J. J. Dannenberg, V. G. Zakrzewski, S. Dapprich, A. D. Daniels, M. C. Strain, O. Farkas, D. K. Malick, A. D. Rabuck, K. Raghavachari, J. B. Foresman, J. V. Ortiz, Q. Cui, A. G. Baboul, S. Clifford, J. Cioslowski, B. B. Stefanov, G. Liu, A. Liashenko, P. Piskorz, I. Komaromi, R. L. Martin, D. J. Fox, T. Keith, M. A. Al-Laham, C. Y. Peng, A. Nanayakkara, M. Challacombe, P. M. W. Gill, B. Johnson, W. Chen, M. W. Wong, C. Gonzalez, J. A. Pople, Gaussian, Inc., Pittsburgh, PA, **2004**.

[18] J. R. Cheeseman, M. J. Frisch, F. J. Delvin, P. J. Stephens, *Chem. Phys. Lett.* **1996**, *252*, 211–220.

Received: October 5, 2009
Published online: March 16, 2010

